A Quasi-Elastic Neutron Scattering Study of the Ammonium Ions in $CsNH_4$–Y Zeolite

W. P. J. H. Jacobs,*,† V. O. de Haan,‡ R. A. van Santen,† and L. A. de Graaf‡

Schuit Institute of Catalysis, Laboratory of Inorganic Chemistry and Catalysis, Eindhoven University of Technology, P.O. Box 513, 5600 MB Eindhoven, The Netherlands, and Interfaculty Reactor Institute, Delft University of Technology, Mekelweg 15, 2629 JB Delft, The Netherlands

*Received: December 3, 1993**

Quasi-elastic neutron scattering has been used to study the reorientation mechanism for ammonium ions in cesium-exchanged zeolite Y. This sample contains ammonium ions preferentially located in the sodalite cages at site I′. These ions reorientate with 120° or 180° jumps around fixed axes through the nitrogen atom. This corresponds to a bonding geometry in which the ammonium ion interacts via three or two hydrogen atoms with the lattice oxygen atoms. Additionally, a reorientation around a fixed axis through two hydrogen atoms of the ammonium ion may occur. The ammonium ion then jumps between two equilibrium positions: one position involves a 2-fold bonding geometry and the other a 3-fold bonding geometry. At 300 K the effective time interval between two jumps is $\tau = 1.2 \pm 0.5$ ps. Compared to zeolite Rho, the ammonium ions in the cesium-exchanged zeolite Y show a more restricted reorientational behavior, resulting in a larger elastic incoherent structure factor.

Introduction

Zeolites are frequently used as acid catalysts in hydrocarbon conversion reactions.[1] The active form is the proton form which can be obtained after heating of ammonium-exchanged zeolites. After desorption of ammonia and coadsorbed water the active sites, the acidic Brønsted sites, are generated. Information on the acid strength of these sites can be obtained from studies on the interaction of the sites with a base. In the case of adsorption or desorption of ammonia, proton transfer occurs. The initial and final species in this reaction, the bridging hydroxyls and the ammonium ions, have been the subject of several spectroscopic studies. Infrared spectroscopy has been used to study the O–H stretching modes of the Brønsted sites and the N–H stretching and bending modes of the ammonium ions.[2-5] The translational modes of the ammonium ions against the zeolite lattice (10–25 meV, 80–200 cm^{-1}) have been studied with far-infrared spectroscopy.[6-8] For zeolite Y these studies resulted in an assignment of the different translational modes to ammonium ions, located at different positions in the supercages and sodalite cages.[8]

Also ^1H MAS NMR has been used to study the acidic sites[9-14] and ammonium ions[15] in zeolites. Recent experiments with this technique indicated different mobilities for ammonium ions located in the supercages and sodalite cages of zeolite Y.[16] These findings are in agreement with inelastic neutron scattering studies on ammonium-containing Y zeolites.[17] Both studies indicate that the ammonium ions located in the sodalite cages are more rigidly bonded to the lattice than those in the supercages.

Quasi-elastic neutron scattering (QENS) can be used to obtain information on reorientation processes of hydrogen-containing compounds.[18,19] So far this technique has not been widely used in the study of ammonium ions in zeolites, although work on ammonium ions in zeolite Rho[20] has been done. In this paper we will study the reorientational motion of ammonium ions in zeolite Y. After partial exchange of the zeolite with cesium ions, the ammonium ions are located exclusively in the sodalite cages near the hexagonal prisms (sites I′ in Figure 1).[3,5,8,16] In this way we can study the reorientational behavior of ammonium ions, which are located in only one type of the cages of zeolite Y, the sodalite cages.

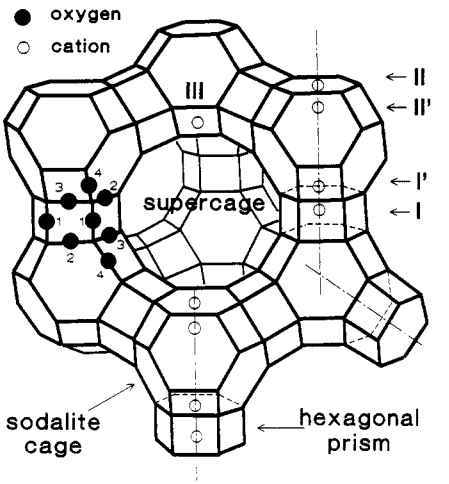

Figure 1. Faujasite structure. The different oxygen atoms are indicated by the numbers 1–4. The different cation positions are indicated by Roman numerals.

Experimental Section

The sample has been obtained by exchanging the ammonium form of zeolite Y (Linde LZ-Y62, Si/Al = 2.4, Na^+/NH_4^+ = 0.2) four times at 353 K in 1 M solutions of NH_4NO_3 and three times at room temperature in 0.3 M solutions of CsCl. According to elemental analyses on silicon, aluminum, sodium, and cesium and Kjeldahl analysis for the determination of the ammonium content, the composition of the sample was $(NH_4)_{18}Na_3Cs_{35}Y$.

For the QENS measurement an anhydrous ammonium-containing sample was used. This sample was obtained by heating in an ampule 20 g of the hydrated zeolite at a rate of 0.2 °C/min in vacuo up to 623 K in order to desorb water and ammonia. After 16-h evacuation at this temperature the zeolite was cooled to room temperature, and 0.01 mol of anhydrous ammonia (UCAR, 99.997% purity) was adsorbed. Then the sample was evacuated for 14 h at 353 K to desorb weakly bonded ammonia, and the ampule was sealed. Finally, in a glovebox filled with dry nitrogen, the sample was transferred to a flat aluminum sample chamber, shielded with cadmium, for the neutron measurements.

The neutron scattering experiments were performed on the rotating-crystal time-of-flight spectrometer at the Delft 2 MW reactor.[21] A pulsed monochromatic neutron beam with a

† Eindhoven University of Technology.
‡ Delft University of Technology.
* Abstract published in *Advance ACS Abstracts*, February 1, 1994.

0022-3654/94/2098-2180$04.50/0

wavelength of $\lambda = 0.238$ nm ($E = 14.4$ meV) was produced by a rotating pyrolytic graphite crystal. Undesired reflections were suppressed by two Fermi choppers, rotating in phase with the crystal. Time-of-flight spectra were obtained simultaneously with 75 ^{3}He detectors (20 cm long and 2.5 cm diameter) arranged at different angles from 3.95° to 85°, covering a wavevector-transfer range of 1.8–36 nm^{-1} at zero energy transfer. Experiments were carried out at 15 and 300 K for the zeolite sample and a vanadium sample. The latter measurement was used to determine the Bragg peak intensities of the sample (see below).

The procedures for data handling have been described in detail elsewhere (section 4.2 of ref 22). These procedures consist of the following steps:

TINO: A linear time-independent background was subtracted from the time-of-flight spectra for the sample, and vanadium measurements and the measured intensities were normalized with respect to the number of incident neutrons. The resolution was determined by the measurement of the sample at 15 K.

DEFF: The time-of-flight spectra are corrected for the detector efficiencies.

INTPOL: The double-differential cross section obtained at the experimental scattering angles is converted to the dynamic structure factor $S(k,\omega)$ at a constant angle and equidistant ω grid.

TOP: The relation between the time-of-flight scale and the wavelength scale is determined.

DECO: This step calculates the Fourier transform $F_i(k,t)$ of $S(k,\omega)$ and corrects for the instrumental resolution. A real (Re) and a imaginary (Im) part are obtained after the transformation. A nonzero Im $F_i(k,t)$ indicates asymmetries in $S_i(k,\omega)$ due to the neglect of imperfections such as multiple scattering, statistics, and the fact that $S(k,\omega)$ was taken at constant angle, rather than at constant k. We will use Re $F_i(k,t)$ only when Im $F_i(k,t)$ is small. In order to improve the statistics, the results for three to five neighboring detectors were summed after executing DECO.

Results

In Figure 2a the time-of-flight spectra at 44° ($k = 19.6$ nm^{-1}) are given for the measurement of the sample at 300 and 15 K. The corresponding Fourier transform $F_i(k,t)$ of $S(k,\omega)$ is shown in Figure 2b. In Figure 3 the total number of neutrons counted for each detector is given for the sample and vanadium measurements. For a pure incoherent scattering sample the ratios of the intensities should be constant for each detector, apart from the effect of Debye–Waller factors. We see that strong Bragg reflections from the zeolite and the sample chamber are present. The first intense reflection corresponds to reflection of the (111) plane of the zeolitic lattice. The detectors at the positions of these strong Bragg reflections are not used for further analyses. Also, weak Bragg reflections are observed at various angles. For larger angles we see a decrease in intensity due to the increasing absorption in the sample.

We will use a simple model[21] for fitting to the real part of the intermediate incoherent scattering function $F_i(k,t)$:

$$\text{Re } F_i(k,t) = \frac{C(k)[A(k) + (1 - A(k))\exp(-t/\tau)] + B(k)}{1 + B(k)}$$

Here A describes the contribution of the elastic scattering, τ is an effective relaxation time for rotational jump diffusion, and $C = e^{-u^2k^2}$ is the Debye–Waller factor at 300 K of the zeolite with u^2 the mean-square translational amplitude of the hydrogen atoms and k the wavevector transfer. In the preceding part, we already mentioned the presence of weak Bragg reflections of the zeolite, which contribute to the elastic scattering. This elastic contribution has to be measured and subtracted. One way to do this is to record the quasi-elastic spectra of the proton zeolite, before adsorption of ammonia. However, the structures of proton and ammonium zeolites differ, since protonation of the zeolite lattice

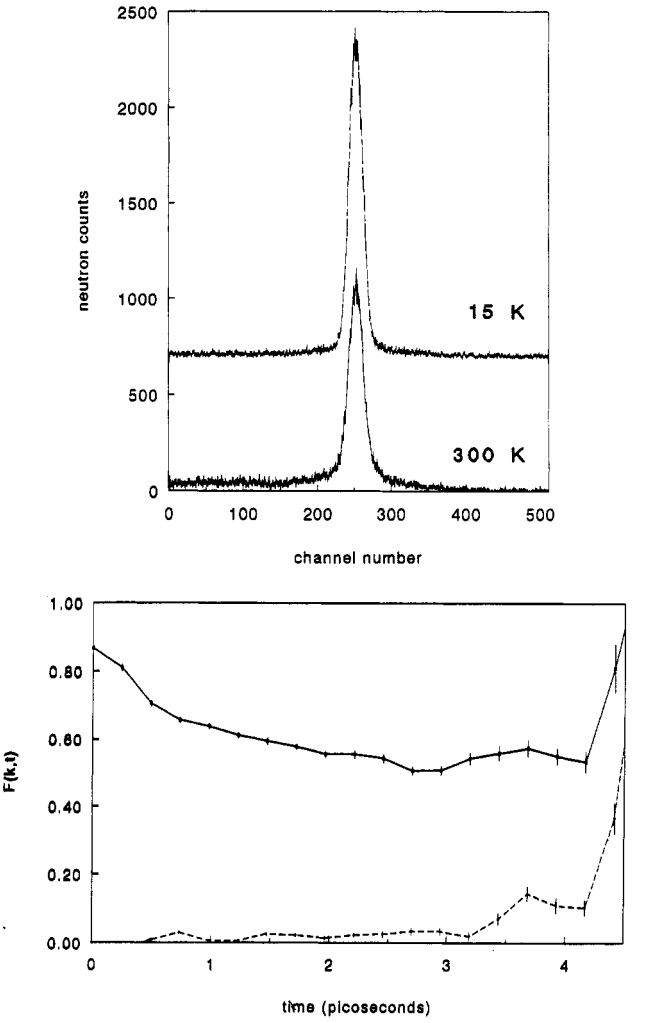

Figure 2. (a) Time-of-flight spectra for the zeolite sample, measured at 300 and 15 K ($\phi = 44°$, $k = 19.6$ nm^{-1}). (b) Real (continuous line) and imaginary (broken line) part of $F_i(k,t)$ for the zeolite sample at 300 K ($\phi = 44°$, $k = 19.6$ nm^{-1}).

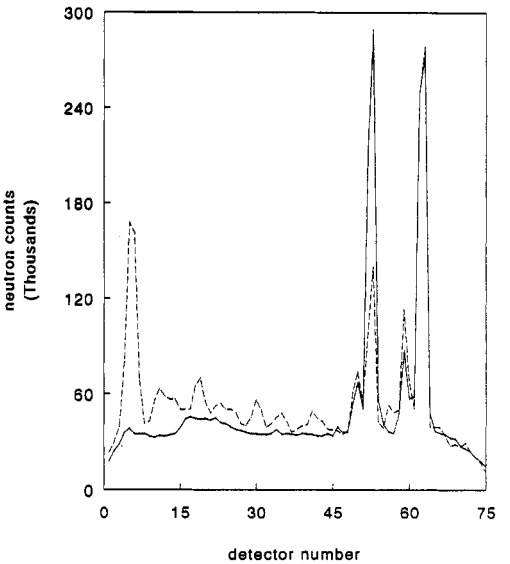

Figure 3. Total neutron intensity for the different detectors for the vanadium measurement (continuous line) and the zeolite measurement (broken line), both at 15 K. Detector 1 corresponds with $\phi = 3.95°$, and detector 75 corresponds with $\phi = 85°$.

results in structural deformations.[23,24] Further, the locations of the acidic protons and the ammonium ions are different. The former are covalently bound to oxygen atoms of the lattice,[5]

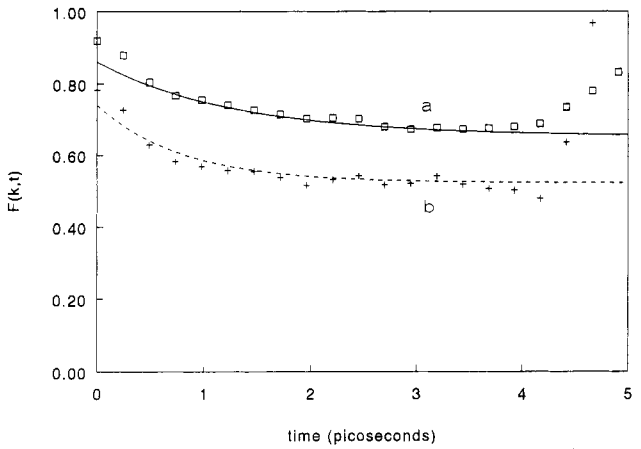

Figure 4. Re $F_i(k,t)$ for the zeolite sample measured at 300 K. Experimental points are obtained after summation of the intensities of neighboring detectors. The curve is the result of the fit. (a) $\phi = 35°$, $k = 15.8$ nm^{-1} (detectors 28–31). Fit: $\tau = 1.3 \pm 0.2$ ps, $A = 0.67 \pm 0.02$, and $u^2 = 0.0008 \pm 0.0001$ nm^2. (b) $\phi = 75°$, $k = 32.3$ nm^{-1} (detectors 65–68). Fit: $\tau = 0.8 \pm 0.2$ ps, $A = 0.69 \pm 0.02$, and $u^2 = 0.0003 \pm 0.0001$ nm^2.

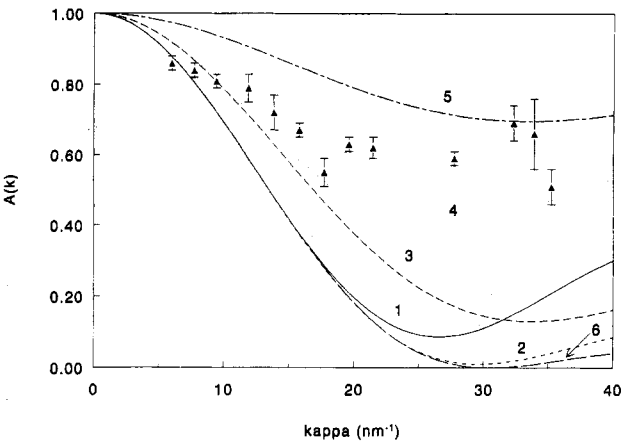

Figure 5. $A(k)$ as a function of k. Experimental points are obtained after fitting the real part of $F_i(k,t)$. The curves belong to the models discussed in the text.

whereas the ammonium ions are located at the different cation positions[6-8] (see Figure 1). As a result, the elastic contribution of the unloaded sample cannot be used to model the weak Bragg reflections of our sample. Using sodium ions, instead of the ammonium ions, eliminates the problem of lattice deformations caused by protonation of the lattice. Differences in the elastic contributions result now from the different coherent cross sections of the ammonium and sodium ions and from differences in the cation positions. Therefore, we use a different approach by introducing the term $B(k)$ to account for the small Bragg reflections of the zeolite (see also ref 25). This term is almost independent of the temperature in our case. The term $B(k)$ was determined by comparing the sample measurement at 15 K to the vanadium measurement at 15 K. The total scattering intensities for the sample $I_s(i)$ and for vanadium $I_v(i)$ are then given by

$$I_s(i) = I_s(1 + B(k_i))a_s(i)$$

$$I_v(i) = I_v a_v(i)$$

where i denotes the detector number, k_i the wavevector transfer for detector i at zero energy transfer, and $a_s(i)$ and $a_v(i)$ are the attenuation factors due to absorption of neutrons in the sample and the vanadium, respectively. The contribution of the weak Bragg reflections is then given by

$$B(k_i) = \frac{I_v}{I_s}\frac{I_s(i)/a_s(i)}{I_v(i)/a_v(i)} - 1$$

The ratio I_s/I_v was determined by comparing the coherent scattering cross section of the whole sample (σ_s^{coh}) to the incoherent scattering cross section of the hydrogen atoms in the sample (σ_s^{inc}), summed for all detectors ($n = 75$):

$$\frac{I_s}{I_v} = \frac{1}{n}\frac{\sigma_s^{inc}}{\sigma_s^{coh} + \sigma_s^{inc}}\sum_{i=1}^{n}\frac{I_s(i)/a_s(i)}{I_v(i)/a_v(i)} = 1.08$$

Using this information, the obtained Re $F_i(k,t)$ have been fitted with respect to $A(k)$ and τ for the different groups of detectors. The region between 0.4 and 4.0 ps has been used for fitting, since for smaller times Re $F_i(k,t)$ contains contributions due to translational modes (10–25 meV, 80–200 cm^{-1}) of the ammonium ions.[8] Two examples of such a fit are shown in Figure 4. From the results of all fits we obtain for the correlation time $\tau = 1.2 \pm 0.5$ ps, and for the mean-square translational amplitude we find $u^2 = 0.0007 \pm 0.0003$ nm^2. In Figure 5 the results of the fits for $A(k)$ are given.

Discussion

Infrared experiments with self-supported discs showed for this sample that after heating for 1 h at 723 K an infrared band near 3550 cm^{-1} was present. This band is assigned to the hydroxyl stretching modes of acidic protons in the sodalite cages.[5] The band belonging to protons in supercages near 3650 cm^{-1} was almost completely absent, confirming that mainly sodalite cage Brønsted sites are formed. So the large cesium cations are mainly located in the supercages, whereas the ammonium ions are forced into the smaller sodalite cages.

The term $A(k)$ is the elastic incoherent scattering function (EISF) and represents the fraction of the total scattering intensity, which is due to elastic scattering. The k dependence of this term is governed by the mechanism for the reorientational motion for the ammonium ions. In the literature models have been derived for different reorientational mechanisms. We will summarize the results for the models which may describe the jump-reorientational mechanism of ammonium ions in cesium-exchanged zeolite Y (see also Figure 5).[21,25-27]

Model 1 describes 120° reorientations at random around 2, 3, or 4 C_3 axes or 180° reorientations at random around 2 or 3 C_2 axes. Then the EISF is given by

$$A(k) = {}^1/_4[1 + 3j_0(kR_{HH})] \quad (1)$$

where $j_0(kR_{HH}) = \sin(kR_{HH})/(kR_{HH})$ is the zero-order spherical Bessel function and R_{HH} is the proton–proton distance in the ammonium ion ($R_{HH} = 0.1689$ nm[28]).

Model 2 describes 90° jumps at random around three C_2 axes:

$$A(k) = \frac{1}{8}\left[1 + 3j_0(kR_{HH}) + 3j_0\left(kR_{HH}\sqrt{\frac{1}{2}}\right) + j_0\left(kR_{HH}\sqrt{\frac{3}{2}}\right)\right] \quad (2)$$

Model 3 describes 90° jumps around a fixed C_2 axis:

$$A(k) = \frac{1}{4}\left[1 + 2j_0\left(kR_{HH}\sqrt{\frac{1}{2}}\right) + j_0(kR_{HH})\right] \quad (3)$$

Model 4 describes reorientations of 120° around one fixed C_3 axis or of 180° around one fixed C_2 axis (see Figure 6):

$$A(k) = {}^1/_2[1 + j_0(kR_{HH})] \quad (4)$$

Model 5 describes jumps around a fixed axis through two

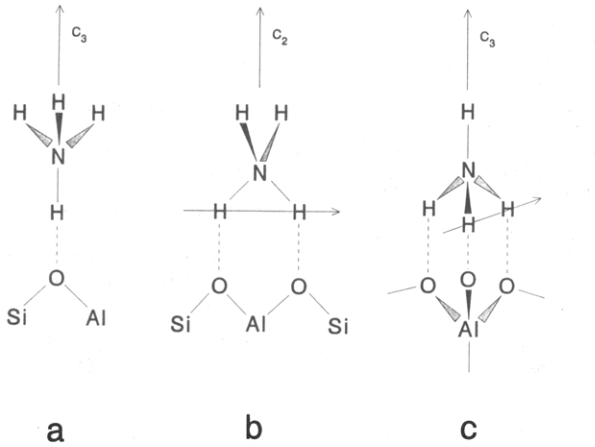

Figure 6. Geometries of the ammonium ions bound to the oxygen atoms of the zeolite lattice. (a) Singly bound. Reorientation can occur around the 3-fold axis (model 4). (b) Doubly bound. Reorientation can occur around the 2-fold axis (model 4) or around the axis through the two hydrogen atoms near the oxygen atoms (model 5). (c) Triply bound. Reorientation can occur adound the 3-fold axis (model 4) or around an axis through two hydrogen atoms near the oxygen atoms (model 5).

hydrogen atoms:

$$A(k) = {}^1/_4[3 + j_0(kR_D)] \quad (5)$$

In this model the nitrogen atom and two hydrogen atoms jump between two equilibrium positions, while the other two hydrogen atoms remain at fixed positions, bonded to the lattice oxygen atoms. Quantum chemical calculations have shown that the ammonium ions are preferentially bonded via two or three hydrogen atoms.[29,30] Model 5 corresponds with jumps between a 2-fold bonding geometry (Figure 6b) and a 3-fold bonding geometry (Figure 6c). Assuming tetrahedral symmetry for the ammonium ion, we calculate for the jump distance R_D a value of 0.1344 nm.[28] This distance corresponds to the movement of one nonbonded hydrogen atom of Figure 6b into the plane through the two bonding hydrogen atoms, which is perpendicular to the C_2 axis, resulting in the geometry of Figure 6c.

For isotropical rotational diffusion, model 6, the following relation is obtained:

$$A(k) = j_0^2\left(kR_{HH}\sqrt{\frac{3}{8}}\right) \quad (6)$$

In Figure 5 the results of these models are compared with the experimentally obtained values for $A(k)$. From this figure we see that the experimental points are in between the curves for models 4 and 5. We conclude that reorientation of the ammonium ions, as measured by QENS, occurs around a fixed axis. However, we cannot discriminate whether this is a reorientation of 120° around a C_3 axis or a reorientation of 180° around a C_2 axis (model 4) or a reorientation around an axis through two protons (model 5). Probably these reorientational mechanisms are all operative. This may be indicative for differences in ordering of the silicon and aluminum of the zeolite framework at the cation sites.

Udovic and co-workers[20] investigated the reorientation mechanism of ammonium ions in zeolite Rho. The locations of these ammonium ions depend on the pretreatment conditions used. In an anhydrous sample of ammonium-exchanged zeolite Rho, as used by Udovic, the ammonium ions are located on the faces of distorted 8-rings.[31] However, when the sample is obtained after readsorption of ammonia onto the proton form of zeolite Rho, one ammonium position is found in the center of the double 8-ring and the other position is outside the double 8-ring in the truncated cubooctahedron.[32] Udovic and co-workers concluded that model 4 gives the best description for the reorientation mechanism. However, they ignored that reorientation about a fixed C_2 axis by 180° is also described by model 4. For the reorientation relaxation time at 300 K they obtained a slightly higher value for zeolite Rho ($\tau \approx 4$ ps). This may be indicative of a slightly higher reorientation barrier for the ammonium ions in zeolite Rho, for which a value of approximately 35 meV was obtained. The presence of the ammonium ions in the 8-rings of zeolite Rho may result in a stronger interaction with the zeolite lattice and a more restricted reorientational behavior as compared to the zeolite Y sample, where the ammonium ions occupy positions in the sodalite cages near the 6-rings.

The librational modes of ammonium ions in zeolite Y and Rho are observed with inelastic neutron scattering.[17,20] For zeolite Rho these modes are observed at 10–14 meV (80–120 cm^{-1}). However, it must be noted that in this region part of the features may also be due to translational modes of the ammonium ions.[8,20] For ammonium ions in the sodalite cages of zeolite Y the librational modes are located near 8 meV (65 cm^{-1}). This value is somewhat lower than found for zeolite Rho. This is in agreement with the shorter reorientation time found in this work. The librational modes for ammonium ions in the supercages are observed at 3–6 meV (24–50 cm^{-1}).[17] So we expect for ions in these cages even a lower barrier for reorientation.

Apart from these slightly hindered librations, more strongly hindered librations are observed at 30–70 meV (240–565 cm^{-1}) for zeolite Y.[17] The ammonium ions in the supercages give again rise to the lower values in this region. These librations correspond to reorientation mechanism with a higher-energy barrier. The corresponding reorientation time τ is longer. However, the resolution of our measurements enables only to resolve the fastest process.

Using results from far-infrared spectroscopy, information about the positions of cations in the zeolitic lattice has been obtained.[6-8] The sodalite cage ammonium ions are located at site I′, where three protons of the ion can interact with three oxygen atoms of one of the six rings of the hexagonal prisms. For such a bonding geometry a reorientation model with reorientations of 120° around a fixed C_3 axis is most likely to occur. The interaction of the ammonium ions with the lattice here occurs via three bonds. This is different from the mechanism adopted by Udovic and co-workers, where the ammonium ions interact only with one bond with the lattice.[20] However, quantum-chemical ab-initio cluster calculations showed that two or three bonds are needed to transfer the proton from the zeolite lattice to the ammonia molecule, forming an ammonium ion.[29,30] The 2-fold bonding geometry may then be obtained from the 3-fold bonding geometry after rotating the ammonium ion around an axis through two hydrogen atoms.

Conclusions

A QENS study of cesium-exchanged zeolite Y with ammonium ions almost exclusively located at site I′ shows that these ions reorientate either with 120° jumps around a fixed C_3 axis or with 180° jumps around a fixed C_2 axis or that these ions jump from a 2-fold bonding geometry to a 3-fold bonding geometry. Except for the model with 180° jumps around the fixed C_2 axis, one or two protons remain at their positions during the reorientation. When the geometry of site I′ is taken into consideration, a mechanism with 120° jumps around a C_3 axis seems to be most likely. Additionally, tumbling of ammonium ions between two equilibrium positions may occur, leaving two hydrogen atoms at fixed positions. The equilibrium positions correspond with a 2-fold and a 3-fold bonding geometry of the ammonium ion. At 300 K the time interval in between two jumps is $\tau = 1.2 \pm 0.5$ ps. For ammonium ions in zeolite Rho a slightly longer time was observed, while for ammonium ions in the supercages of zeolite Y a slightly shorter time is expected. These differences are due to differences in the reorientation barriers, caused by differences in bonding interactions of the ammonium ions with the lattice. Compared

to zeolite Rho, the ammonium ions in the cesium-exchanged zeolite Y studied are more rigidly bound to the lattice. This results in a larger EISF, since on an average the hydrogen atoms in the ammonium ions are less mobile. Apart from the reorientational motions observed here, other reorientations are present which could not be resolved. These reorientations have a much higher barrier for reorientation, and the corresponding residence time between two jumps is longer. For a more detailed analysis, including studies of the energy barriers for reorientation, temperature-dependent experiments on spectrometers with a range of resolutions (i.e., observation times) are necessary.

Acknowledgment. We thank Dr. A. A. van Well for the helpful discussions and advice during this work, and further we are grateful to Mr. J. H. M. C. van Wolput for assistance with the infrared measurements.

References and Notes

(1) Jacobs, P. A. *Carboniogenic Activity of Zeolites*; Elsevier Scientific Publishing: Amsterdam, 1977.
(2) Ward, J. W. *J. Catal.* **1967**, *9*, 225.
(3) Ward, J. W. *J. Phys. Chem.* **1969**, *73*, 2086.
(4) Uytterhoeven, J. B.; Christner, L. G.; Hall, W. K. *J. Phys. Chem.* **1969**, *69*, 2117.
(5) Jacobs, P. A.; Uytterhoeven, J. B. *J. Chem. Soc., Faraday Trans. 1* **1973**, *69*, 359, 373.
(6) Ozin, G. A.; Baker, M. D.; Helwig, K.; Godber, J. *J. Phys. Chem.* **1985**, *89*, 1846.
(7) Baker, M. D.; Ozin, G. A.; Godber, J. *Catal. Rev.—Sci. Eng.* **1985**, *27*, 591.
(8) Ozin, G. A.; Baker, M. D.; Godber, J.; Gil, C. J. *J. Phys. Chem.* **1989**, *93*, 2899.
(9) Freude, D.; Fröhlich, T.; Hunger, M.; Pfeifer, H.; Scheler, G. *Chem. Phys. Lett.* **1983**, *98*, 263.
(10) Freude, D.; Hunger, M.; Pfeifer, H.; Scheler, G.; Hoffman, J.; Schmitz, W. *Chem. Phys. Lett.* **1984**, *105*, 427.
(11) Pfeifer, H.; Freude, D.; Hunger, M. *Zeolites* **1985**, *5*, 274.
(12) Freude, D.; Hunger, M.; Pfeifer, H.; Schwieger, W. *Chem. Phys. Lett.* **1986**, *128*, 62.
(13) Freude, D.; Hunger, M.; Pfeifer, H. *Z. Phys. Chem. (Munich)* **1987**, *152*, 171.
(14) Ernst, H.; Freude, D.; Hunger, M.; Pfeifer, H.; Seiffert, B. *Z. Phys. Chem. (Leipzig)* **1987**, *268*, 304.
(15) Vega, A. J.; Luz, Z. *J. Phys. Chem.* **1987**, *91*, 365.
(16) Jacobs, W. P. J. H.; de Haan, J. W.; van de Ven, L. J. M.; van Santen, R. A. *J. Phys. Chem.* **1993**, *97*, 10394.
(17) Jacobs, W. P. J. H.; van Santen, R. A.; Jobic, H. *J. Chem. Soc., Faraday Trans.*, submitted.
(18) Press, W. *Single-Particle Rotations in Molecular Crystals*; Springer Tracts in Modern Physics, Vol. 92; Springer-Verlag: Berlin, 1981.
(19) Beé, M. *Quasi-elastic Neutron Scattering*; Adam Hilger: Bristol, 1988.
(20) Udovic, T. J.; Cavanagh, R. R.; Rush, J. J.; Wax, M. J.; Stucky, G. D.; Jones, G. A.; Corbin, D. R. *J. Phys. Chem.* **1987**, *91*, 5968.
(21) Steenbergen, C.; de Graaf, L. A.; Bevaart, L.; Bartolome, J.; de Jongh, L. J. *J. Chem. Phys.* **1979**, *70*, 1450.
(22) Verkerk, P.; van Well, A. A. *Nucl. Instrum. Methods Phys. Res.* **1985**, *228*, 438.
(23) van Santen, R. A.; de Man, A. J. M.; Jacobs, W. P. J. H.; Teunissen, E. H.; Kramer, G. J. *Catal. Lett.* **1991**, *91*, 273.
(24) van Santen, R. A.; de Man, A. J. M.; Kramer, G. J. *Zeolite Microporous Solids: Synthesis, Structure and Reactivity*; Derouane, E. G., Lemos, F., Naccache, C., Ramôa Ribeiro, F., Eds.; Kluwer Academic Publishers: Dordrecht, 1992; p 493.
(25) Richardson, R. M.; Howard, J. *Chem. Phys.* **1984**, *86*, 235.
(26) Prask, H. J.; Trevino, S. F.; Rush, J. J. *J. Chem. Phys.* **1975**, *62*, 4156.
(27) Steenbergen, C.; de Graaf, L. A. *Physica B* **1979**, *96*, 1.
(28) *Handbook of Chemistry and Physics*, 62nd ed.; Weast, Ed.; The Chemical Rubber Co.: Cleveland, OH, 1981–82. Assuming tetrahedral symmetry of the ammonium ion, the proton–proton distance R_{HH} is calculated from the proton–nitrogen distance R_{NH} = 0.1034 nm.
(29) Teunissen, E. H.; Duijneveldt, F. B.; van Santen, R. A. *J. Phys. Chem.* **1992**, *96*, 366.
(30) Teunissen, E. H.; van Santen, R. A.; Jansen, A. P. J.; van Duijneveldt, F. B. *J. Phys. Chem.* **1993**, *97*, 203.
(31) McCusker, L. B. *Zeolites* **1984**, *4*, 51.
(32) Fisher, R. X.; Baur, W. H.; Shannon, R. D.; Parise, J. B.; Faber, J.; Prince, E.; *Acta Crystallogr.* **1989**, *C45*, 983.